

Evaluation of an Active Steering System

ADRIAN RODRIGUEZ OROZCO



**KTH Signals
Sensors and Systems**

Master's Degree Project
Stockholm, Sweden 2004

IR-RT-EX-0422

Preface

The author of this report would like to thank the Division of Vehicle Dynamics at The Royal Institute of Technology (KTH) for the opportunity to do this master thesis. The examiner of this thesis is associate professor Karl Henrik Johansson at the Automatic Control Group at the S3 department of KTH.

The master thesis is the final work in my electro technical M. Sc. engineering education at KTH, Stockholm Sweden.

All the discussion with and help from the staff of the division has been very helpful and educating. Special thanks to professor Annika Stensson who arranged a presentation at GM/Saab in Trollhättan. Special thanks also to Markus Agebro, my supervisor, for being available all the time.

I would also like to thank Johan Andreasson and Jonas Jarlmark from the division for sharing their knowledge and supporting me throughout the work.

Abstract

A steering aid system called active steering is evaluated by simulating different driving events. The active steering solution, which is taken from a scientific paper, has been implemented in Matlab/Simulink. A vehicle model, also implemented in Matlab/Simulink, is used to form a total system and to compare the two systems: a conventional vehicle and a controlled vehicle.

The input to the vehicle model is the steering wheel angle performed by the driver. Simulations are made for a constant speed and a specific changeable road adhesion coefficient. The control system takes the yaw rate as input and derives a steering angle contribution to be added to the drivers command.

The motivation for this work is to understand and characterize the response of a vehicle with a complementary steering system. Specific driving events are considered for the simulations such as a wind force disturbance and a severe double lane change.

The response of the controlled vehicle is similar to the response of the conventional vehicle for nominal driving, but the steering aid system reduces the effect of wind force disturbances. Improved stability is obtained for the vehicle during slippery road driving.

Table of content

1 Introduction	1
1.1 Problem formulation	1
1.2 Thesis Outline	2
2 Background	3
2.1 BMW-Active Steering	3
2.2 Quadrasteer	4
3 System description	5
4 Vehicle model	7
4.1 The single-track model	8
4.2 Wheel model	9
4.2.1 Derivation of the tyre slip angle	10
4.2.2 Lateral forces	11
4.2.3 Linearization of the lateral force	12
4.3 Non-linear model	14
5 Control system	15
5.1 Feedback	15
5.2 Feedforward	17
6 Simulations	18
6.1 Conditions for the simulations	18
6.1.1 Driver reaction time	19
6.2 Wind force disturbance	19
6.2.1 Wind force model	19
6.2.2 Wind gust disturbance on vehicle	20
6.2.3 Driver in the loop	22
6.3 Severe double lane change	24
6.3.1 Nominal condition	26
6.3.2 High speed	27
6.3.3 Low friction	28
6.4 Wind force disturbance and variable changes	29
7 Conclusion	31
8 References	34
Glossary	35

1 Introduction

This master thesis is based on two articles [1][8] with a proposed solution of a control system for the steering of a car. The solution has to be implemented and driving events simulated. There are a lot of research and development in the area of steering and steer-by-wire (SBW). The main reason for this is the aim to improve safety and handling. However it is still difficult to value the improvements. In this thesis one solution is implemented and analysed.

An active steering system is a complementary system for a front-steered vehicle that adds or subtracts a component to the steering signal performed by the driver. The steering signal from the driver is an angular movement on the steering wheel. The resulting steering angle is thus composed by the component performed by the driver and the component contributed by the steering system.

1.1 Problem formulation

The aim of the thesis is to reproduce the work in the articles [1][8] and to make a set of simulations to determine whether the predefined goals are fulfilled. Amongst the simulations that are made, events such as wind force disturbances are analysed and input from real driving experiment such as the ISO-standardized double lane change are analysed. The manoeuvres will be simulated for different speeds and road adhesions. Implementation of the system will be made in Matlab/Simulink. All the simulations will be made in Simulink.

The assignment for the master thesis is to implement a steering aid system taking driver action as input. A vehicle model is implemented and the total system including the active steering system is simulated for different driver events. Some focus is laid on the effect of driver reactions due to disturbances.

The goals are to:

- Characterise the difference of the response between the controlled and the uncontrolled vehicle for nominal driving and at the limit driving.
- Establish whether the system is considered to act within driver reaction time.
- Have a system with steady state rejection or attenuation of input disturbances.
- Prove enhancement of the stability region.

1.2 Thesis Outline

The report has the following outline.

Chapter 1 An introduction to the subject and a formulation of the objectives.

Chapter 2 A summarize of the literature survey about steering systems.

Chapter 3 A description of the control system together with the vehicle model. Some of the signals in the system are defined and explained.

Chapter 4 A derivation of the vehicle model, both the linear and non-linear model.

Chapter 5 The control system is analysed and described.

Chapter 6 The simulations are described and responses are depicted.

Chapter 7 Conclusions and results are shown

Chapter 8 Reference list and Glossary.

2 Background

Active Steering is a steering aid system integrated in cars. We are beginning to see different brands with different solutions on the market. The idea is to improve safety and comfort by improved stability and handling. Although the regulations demand a mechanical connection between the steering wheel and the steering rack, actuators are used to influence the mechanical system.

The following section will describe some of the technical solutions of the steering systems used today. Solutions used by BMW (Active Steering) and General Motors (QuadraSteer) will be considered.

Articles on Active Steering have been studied. The survey focus has been on the automatic control area and on the steer-by-wire development. Active steering is the idea of an integrated steering support system for cars. The system has to behave like the steering on conventional cars but with additional functionality such as disturbance rejection due to, for example, μ -split (split adhesion coefficient between wheels), wind gusts or decreased road adhesion conditions. Several existing systems are conceptual and not intended for the market, but for example BMW has a semi-mechanical system installed on the 530-cars.

The two systems explained below are different examples on how to change the conventional steering of a car. The most important reason for changing the steering characteristics of a car is to improve safety and comfort. The following sections will describe a specific theoretical solution for a steering system.

2.1 BMW-Active Steering

The system that BMW uses has a speed dependent variable steering ratio and also the ability to adjust for disturbances during driver reaction time [12]. This is achieved with a planetary gear with two inputs and one output and a fast transmission of information (100 Hz) from different sensors. The planetary gear is able to add or subtract a signal from the response of the steering wheel that controls the tyre wheel angle. The planetary gear is situated between the steering wheel and the conventional steering rack as shown in Figure 1.



Figure 1: *The placement of the planetary gear and the electric motor [12].*

In the BMW Active Steering system the sun gear is the input and the planet carrier is the output. The ring gear that also is input is controlled by an electric motor steered by a computer. If the ring gear is held fixed then the steering ratio is constant and only dependent on the steering wheel. But if the ring gear is in motion at the same time as the steering wheel a variable steering ratio is attained. In some situations the ring gear increases the response of the steering wheel, in other situations the response decreases.

At low speed the planetary gear adds a contribution to the steering angle, which makes the steering wheel lock-to-lock positions less than two rounds on the steering wheel. This is advantageous in parking situations and other slow moving situations since the driver can maintain the grip on the steering wheel. At high speed the planetary gear subtracts a contribution to the steering angle and between the steering wheel lock-to-lock positions it is about four rounds. This increases the safety for evasive manoeuvres on the steering wheel and it provides an increased precision at highway driving.

2.2 Quadrasteer

Another system on the market is the Quadrasteer system used by General Motors. This is also a complement to the conventional steering system. Quadrasteer supplements, for the moment, pick-up trucks with an electronic rear-wheel steering system. The functionality of the Quadrasteer works in three main phases; negative, neutral and positive.

The negative phase acts during low speed. During this phase the rear wheels turn in the opposite direction of the front wheel pair. This makes trailers follow the true vehicle path more closely for reversing and parking situations and decreases the turning circle diameter.

At moderate speeds the neutral phase takes affect. This means that the rear wheels are kept straight and the total steering will be the same as a conventional vehicle.

The positive phase acts at high speed travelling. The rear wheels turn in the same way as the front wheels to add vehicle stability. This is achieved by reducing the vehicle yaw required to accomplish a manoeuvre as lane change or evasive manoeuvres [11].

3 System description

The system described in Figure 2 is a control system developed by the authors of [1]. The input signal to the system u_d is the steering angle set by the driver. In ordinary vehicles there is a constant ratio between the steering wheel angle and the tyre angle. Thus u_d is equal to δ_d / R where R is the characteristic steering gear ratio and δ_d is the steering wheel angle. The objective of the technical solution is to obtain improved vehicle handling. This is particularly important during high speed and/or low road adhesion. The total steering angle, expressed in Figure 2 by u , is compound by the signal from the driver and an additional steering angle δ_c from the control system:

$$u = u_d + \delta_c$$

The controller has a feedforward $K1$ and a feedback $K2$. Then it is possible to write the expression for δ_c as

$$\delta_c = K2 \cdot r - K1 \cdot K2 \cdot u_d$$

Only the yaw rate is used for the feedback so according to [1] the control system is theoretically possible to implement in an electrically steered vehicle. Equipment for measuring the speed, the yaw rate and the steering wheel angle is needed and of course an actuator and its mechanical device for contributing the additional steering angle.

The second input to the vehicle is the side wind force with a predefined action point, which is assumed to act 0.4 meters in front of the centre of gravity on the right side of the car. This influence can be modelled in various ways. In this work the wind is modelled as suggested in [7], this is briefly described in section 6.2.

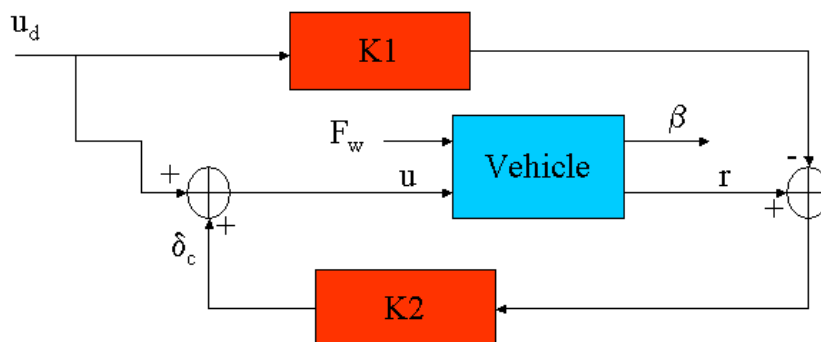


Figure 2: A description of the complete system

The vehicle model is developed in two versions, a linear model where the lateral forces are approximated as linear relationships, and a non-linear model.

3 System description

Table 1 and 2 contains the nomenclature used in the thesis and all the different parameters and their values. Some of the key terms used in the report are listed and explained in a glossary at the end of the report.

G	Vehicle centre of gravity (CoG)
m	Mass (991 kg)
J	Inertia (1574 kg m ²) in yaw direction
L _f	Distance from CoG to front axle (1 m)
L _r	Distance from CoG to rear axle (1.46 m)
s _b	Track width (1.4 m)
R	Steering gear ratio (21)
C _f	Front cornering stiffness (41.6 kN/rad)
C _r	Rear cornering stiffness (47.13 kN/rad)
μ	Road adhesion value between 0 and 1

Table 1: *Nomenclature of the included parameters*

n _t	Tyre road length contact (1.3 cm)
F _{xi} , F _{yi}	Longitudinal and lateral forces of the i:th tyre (N)
F _{xf} , F _{yf}	Total front longitudinal and lateral force (N)
F _{xr} , F _{yr}	Total rear longitudinal and lateral force (N)
α _i	Slip angle of the i:th tyre (rad)
w = F _w	Wind force (N)
L _w	Distance of wind force action (0.4 m)
k _x , k _y	Air drag coefficient (kg/m)
(v _x , v _y)	CoG speed in vehicle frame (m/s)
β	Vehicle side slip angle (rad)
r	Yaw rate (rad/s)
u = δ _f	Steering angle (rad)

Table 2: *Nomenclature of the included parameters*

4 Vehicle model

This chapter will describe the linear vehicle model used for controller analysis and the non-linear model used for the simulations. The final linear vehicle model will be a single-track model (bicycle) with the steering angle, performed by the driver, as a control signal. A crosswind gust will be a disturbance input to the vehicle model. The output of the model will be β , the sideslip angle, and, r the yaw rate, see the glossary at the end for explanations.

The vehicle model is derived from the equations of motion of a front steered 4-wheel vehicle. Figure 3 shows the parameters involved and their definition. The positive x-axis starts at the centre of gravity and points in the forward direction of the vehicle. This direction is also referred to as the longitudinal direction. The y-axis corresponds to the lateral direction and starts from the centre line. As shown in Figure 3 the centre of gravity (CoG) is located on the centre line but closer to the front axle than to the rear axle. At a short distance (L_w) from the centre of gravity is an action point of a disturbance wind force defined; its direction is parallel to the lateral direction. Since lateral control is concerned in this thesis motions such as roll, bounce and pitch are neglected (see the glossary for definitions). The front wheel pair is assumed to have the same steering angle.

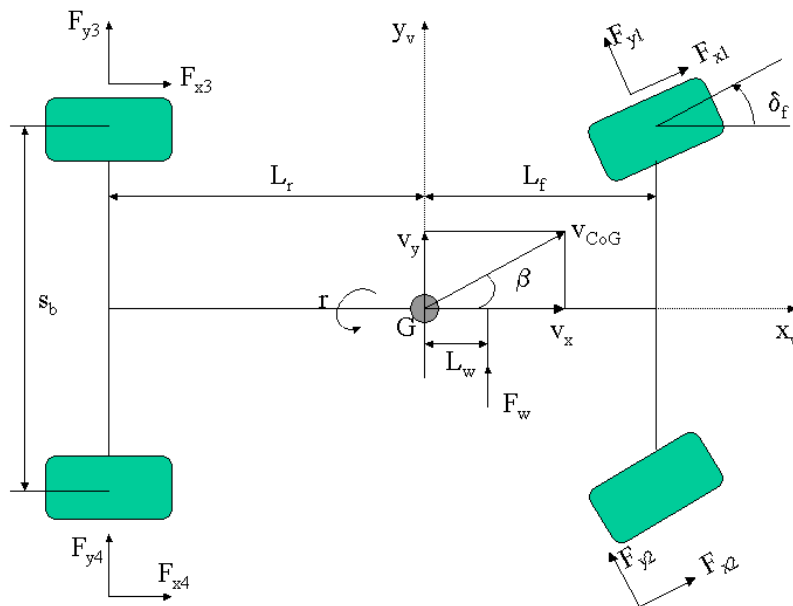


Figure 3: *Definitions of a front steered vehicle*

The expressed forces and parameters in Figure 3 will be used in the next chapter for the derivation of the vehicle model.

4.1 The single-track model

Since the final model will be a linear single-track model a few approximations and simplifications will be made. For simplicity the lateral forces of each wheel pair are added into one force; F_{xf} for the front axle and for the rear axle F_{xr} . The same is done for the longitudinal forces F_{yf} and F_{yr} . For the torque in the system the resulting forces ΔF_f and ΔF_x are needed. Notice that ΔF_x is approximately zero. The equations defining the forces are

$$\begin{aligned} F_{xf} &= F_{x1} + F_{x2} & F_{yf} &= F_{y1} + F_{y2} & \Delta F_f &= F_{y2} - F_{y1} \\ F_{xr} &= F_{x3} + F_{x4} & F_{yr} &= F_{y3} + F_{y4} & \Delta F_x &= (F_{x4} - F_{x3}) + (F_{x2} - F_{x1}) \cdot \cos \delta_f \end{aligned} \quad (1)$$

Writing the translational and the rotational equations of motion yields a non-linear system equation (2). The coordinate system of the equations is the vehicle coordinate system i.e. the vehicle frame. A transformation of the coordinate system has to be made to be able to follow the vehicle track in the road frame (the inertial coordinate system).

$$\begin{cases} m(\dot{v}_x - v_y \cdot r) = F_{xf} \cdot \cos \delta_f + F_{xr} - F_{yf} \cdot \sin \delta_f - k_x \cdot v_x \cdot |v_x| \\ m(\dot{v}_y + v_x \cdot r) = F_{xf} \cdot \sin \delta_f + F_{yr} + F_{yf} \cdot \cos \delta_f - k_y \cdot v_y \cdot |v_y| + F_w \\ J \cdot \dot{r} = L_f (F_{xf} \cdot \sin \delta_f + F_{yf} \cdot \cos \delta_f) - L_r \cdot F_{yr} + \frac{s_b}{2} (\Delta F_x - \Delta F_f \cdot \sin \delta_f) + L_w \cdot F_w \end{cases} \quad (2)$$

Since the first row describes the motion in longitudinal direction it will be ignored because only the lateral stability is of interest in this case. By using the approximation for small angles, $(\cos(x), \sin(x)) \approx (1, x)$, and reshaping the expression, the equation of motion can approximately be written as

$$\begin{cases} \dot{v}_y = \frac{1}{m} (F_{xf} \cdot \delta_f + F_{yr} + F_{yf} - k_y \cdot v_y \cdot |v_y| + F_w - v_x \cdot r) \\ \dot{r} = \frac{1}{J} \left(L_f (F_{xf} \cdot \delta_f + F_{yf}) - L_r \cdot F_{yr} + \frac{s_b}{2} (\Delta F_x - \Delta F_f \cdot \delta_f) + L_w \cdot F_w \right) \end{cases} \quad (3)$$

For simplicity, we write v_x as v in the sequel. The chosen states for the state space system are $\beta = v_y / v$ and r . The derivative of β is then equal to $\dot{\beta} = \dot{v}_y / v$. The nominal velocity for the system is set to 20 m/s. When the track width s_b is neglected in equation (3) a single-track model is given, Figure 4.

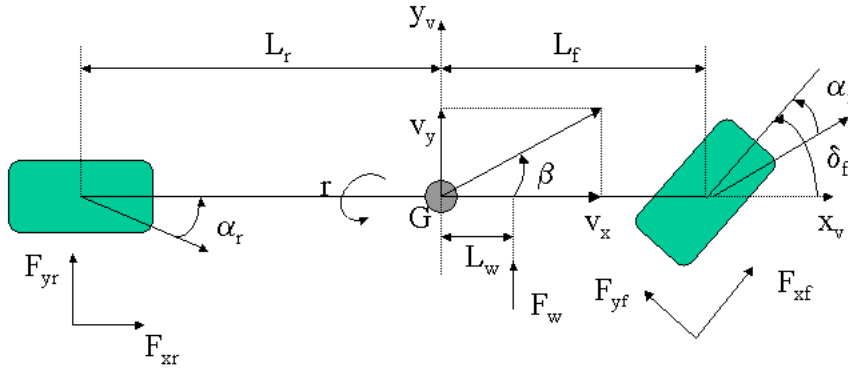


Figure 4: Definitions of a single-track model.

4.2 Wheel model

This part will explain the lateral and longitudinal forces used in section 4.1. In the contact between tyre and track friction forces and normal forces will arise. F_{xi} and F_{yi} are friction forces on each tyre ($i = 1,2,3,4$) of a four-wheel vehicle. There are different ways to compute these forces. The longitudinal forces F_{xi} depend on the longitudinal slip at each tyre while the lateral force on every wheel is a function of the corresponding tyre slip angle α_i , the tyre slip angle is described later on.

Because of the assumption of small angles ($\delta_f \ll 1$) the influence of the lateral component of the longitudinal force F_{xf} in equation (3) will be neglected. The lateral forces are functions of the corresponding slip angles

$$F_{yf} = F_{yf}(\alpha_f) \quad \text{and} \quad F_{yr} = F_{yr}(\alpha_r)$$

The slip angles are expressed by:

$$\alpha_f = \alpha_1 = \alpha_2 = \delta_f - \arctan\left(\beta + \frac{L_f \cdot r}{v}\right) \approx \delta_f - \beta - \frac{L_f \cdot r}{v}$$

$$\alpha_r = \alpha_3 = \alpha_4 = -\arctan\left(\beta - \frac{L_r \cdot r}{v}\right) \approx -\beta + \frac{L_r \cdot r}{v}$$
(4)

4.2.1 Derivation of the tyre slip angle

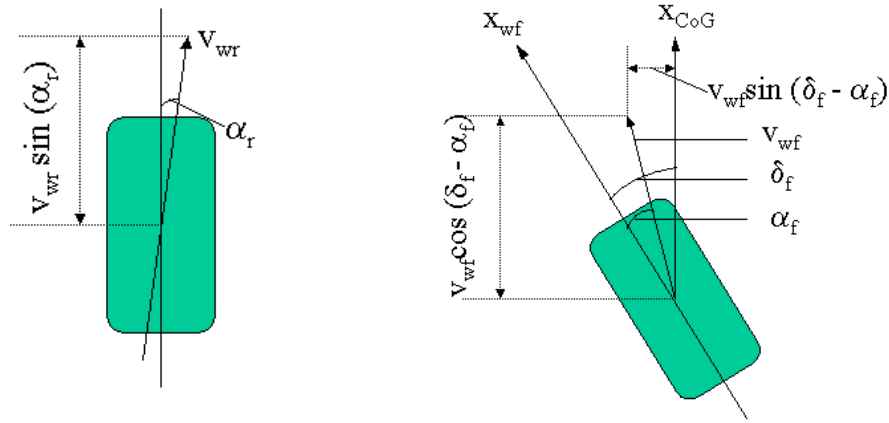


Figure 5: Definitions of the rear (left) and front (right) wheel.

A velocity balance equation can be formed according to the definitions in Figure 5. The term v_{wf} describes the direction of the front wheel velocity. The chassis and the wheels have identical velocity at the wheel ground contact point [2].

So for the **front** wheel in the lateral direction the expression for the velocities are

$$\underbrace{v_{wf} \cdot \sin(\delta_f - \alpha_f)}_{\text{wheel velocity}} = \underbrace{L_f \cdot r + v \cdot \sin(\beta)}_{\text{chassis velocity}} \quad (5)$$

The expression for corresponding velocity in the longitudinal direction is

$$v_{wf} \cos(\delta_f - \alpha_f) = v \cdot \cos(\beta) \quad (6)$$

Dividing equation (5) with equation (6) actually yields the lateral velocity divided with the longitudinal velocity

$$\tan(\delta_f - \alpha_f) = \frac{L_f \cdot r + v \cdot \sin(\beta)}{v \cdot \cos(\beta)} \quad (7)$$

Assuming small angles finally yields the expression as (4)

$$\delta_f - \alpha_f \approx \arctan\left(\frac{L_f \cdot r}{v} + \beta\right) \approx \frac{L_f \cdot r}{v} + \beta \quad (8)$$

For the rear wheel the expression is

$$\tan(\alpha_r) = \frac{L_r \cdot r - v \cdot \sin(\beta)}{v \cdot \cos(\beta)} \quad (9)$$

This yields for small angles

$$\alpha_r \approx -\beta + \frac{L_r \cdot r}{v} \quad (10)$$

4.2.2 Lateral forces

One approach for expressing the lateral forces is the semi empirical so-called magic formula of Pacejka [4] expressed below (11). This is the lateral force for each wheel.

The coefficients B_i , C_i , D_i and E_i depend on the characteristics of the tyre, the road condition and on the vehicle operational condition [1]. Table (3) shows the coefficient values used for this vehicle when the road adhesion is assumed to be high ($\mu = 1$).

$$F_{y_i}(\alpha_i) = D_i \cdot \sin\left[C_i \cdot \arctan\left\{B_i(1 - E_i) \cdot \alpha_i + E_i \cdot \arctan(B_i \cdot \alpha_i)\right\}\right] \quad (11)$$

Tire	B_i	C_i	D_i	E_i
Front ($i = 1,2$)	8.3278	1.1009	2268	-1.661
Rear ($i = 3,4$)	11.6590	1.1009	1835.8	-1.542

Table 3: Pacejka wheel parameters

To be able to simulate the system for different road adhesion coefficients μ has to be incorporated to the Pacejka parameters. If μ is considered a variable in the range [0 1], where $\mu=0.2$ is considered an icy road and $\mu=1$ is considered a dry road, it is possible to change the parameters to $B_i = B_i \cdot (2 - \mu)$ and $C_i = C_i \cdot (5/4 - \mu/4)$ and $D_i = D_i \cdot \mu$. Figure 6 shows the lateral force of the front tyre as a function of the slip angle α .

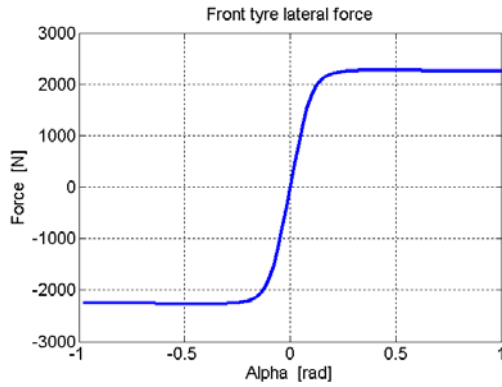


Figure 6: Lateral force of a front tyre.

4.2.3 Linearization of the lateral force

The linearization, of (11), is done around $\alpha_i = 0$. For F_{y1} the calculations are

$$F_{y1} \approx F_{y1}(0) + \frac{\partial F_{y1}(0)}{\partial \alpha_1} \cdot (\alpha_1 - 0) \dots \quad (12)$$

Since the first term in equation (12) is zero the expression for the evaluated derivation is

$$F_{y1} \approx (\alpha_1) \left(D_1 C_1 \left(\left(B_1 (1 - E_1) + E_1 \frac{B_1}{1 + (B_1 \cdot \alpha_1)^2} \right) \cos(C_1 \arctan(B_1 (1 - E_1) \alpha_1 + E_1 \arctan(B_1 \alpha_1))) \right) \right) \Bigg|_{\alpha_1=0}$$

If the value zero is inserted for α_1 the expression is simplified to

$$F_{y1} \approx D_1 \cdot C_1 \cdot B_1 \cdot (\alpha_1)$$

Thus the resulting lateral forces simplifies to the following expressions for small α_i

$$\begin{aligned} F_{y1}(\alpha_1) &= (D_1 \cdot C_1 \cdot B_1) \cdot \alpha_1 & F_{y3}(\alpha_3) &= (D_3 \cdot C_3 \cdot B_3) \cdot \alpha_3 \\ F_{y2}(\alpha_2) &= (D_2 \cdot C_2 \cdot B_2) \cdot \alpha_2 & F_{y4}(\alpha_4) &= (D_4 \cdot C_4 \cdot B_4) \cdot \alpha_4 \end{aligned} \quad (13)$$

The front cornering stiffness C_f and the rear cornering stiffness C_r (see glossary) can be expressed as

$$\frac{C_f}{2} = D_1 \cdot C_1 \cdot B_1 = D_2 \cdot C_2 \cdot B_2 \quad \frac{C_r}{2} = D_3 \cdot C_3 \cdot B_3 = D_4 \cdot C_4 \cdot B_4 \quad (14)$$

By using the equations (1), (4), (13) and (14) the lateral forces can be written as

$$F_{yf}(\alpha_f) = F_{y1} + F_{y2} = \frac{C_f}{2} \cdot \alpha_f + \frac{C_f}{2} \cdot \alpha_f = C_f \cdot \alpha_f = C_f \cdot \left(\delta_f - \beta - \frac{L_f \cdot r}{v} \right)$$

$$F_{yr}(\alpha_r) = F_{y3} + F_{y4} = -C_r \cdot \left(\beta - \frac{L_r \cdot r}{v} \right) \quad (15)$$

If expression (15) is used in equation (3) and the term including the air drag coefficient is neglected the state space system of the vehicle model can be expressed as

$$\dot{x} = Ax + Bu \quad B = [B_w \quad B_u]$$

with state vector $x = [\beta, r]^T$ and the vector $u = [w, u]^T$, the disturbance input $w = F_w$ and the control input $u = \delta_f$.

$$A = \begin{bmatrix} -\frac{C_r + C_f}{m \cdot v} & -1 + \frac{L_r \cdot C_r - L_f \cdot C_f}{m \cdot v^2} \\ \frac{L_r \cdot C_r - L_f \cdot C_f}{J} & -\frac{L_r^2 \cdot C_r + L_f^2 \cdot C_f}{J \cdot v} \end{bmatrix} \quad B_w = \begin{bmatrix} 1 \\ \frac{m \cdot v}{L_w} \\ J \end{bmatrix} \quad B_u = \begin{bmatrix} \frac{C_f}{m \cdot v} \\ \frac{C_f \cdot L_f}{J} \end{bmatrix} \quad (16)$$

4.3 Non-linear model

The non-linear model is developed with the lateral and rotational part of equation (2) together with the non-linear expression of the lateral forces equation (11). The formula of the tyre slip angles below is the input to equation (11). The model is built up in Simulink.

$$\alpha_1 = \delta_f - \arctan \left(\frac{v_y - (n_t \cos \delta_f) \cdot \dot{\delta}_f - (n_t \cos \delta_f - L_f) \cdot r}{v + (n_t \sin \delta_f) \cdot \dot{\delta}_f + \left(n_t \sin \delta_f - \frac{s_b}{2} \right) \cdot r} \right)$$

$$\alpha_2 = \delta_f - \arctan \left(\frac{v_y - (n_t \cos \delta_f) \cdot \dot{\delta}_f - (n_t \cos \delta_f - L_f) \cdot r}{v + (n_t \sin \delta_f) \cdot \dot{\delta}_f + \left(n_t \sin \delta_f + \frac{s_b}{2} \right) \cdot r} \right)$$

$$\alpha_3 = -\arctan \left(\frac{v - L_r \cdot r}{v - \frac{s_b \cdot r}{2}} \right)$$

$$\alpha_4 = -\arctan \left(\frac{v - L_r \cdot r}{v + \frac{s_b \cdot r}{2}} \right)$$

Table 4: Non-linear tyre slip angles [1]

Figure 7 below shows the discrepancy between the linear and the nonlinear vehicle model. The left plot shows the yaw rate for a severe double lane change and the right plot shows the yaw rate for a wind gust disturbance.

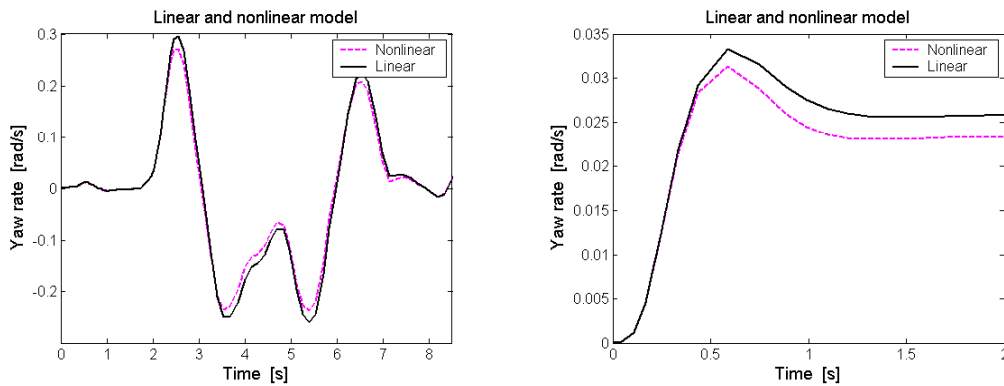


Figure 7: Yaw rate for the linear and nonlinear model for two cases.

5 Control system

The control system is composed of a feedback and a feedforward part. The method used for computing the controller is H_∞ optimisation [11][6]. First the feedback part is developed to ensure robust stability and to reject step disturbances on the yaw rate [1]. Then the feedforward part makes the system fast enough and ensures the same steady state value as the conventional car.

By referring to Figure 2 it is clear that the transfer function of the vehicle is a 2x2-transfer matrix G , two inputs and two outputs. The transfer function from the steering angle to the yaw rate is called G_{22} , and it is a proper and stable transfer function. The question of stability and robustness of the system depicted in Figure 2 is investigated in this chapter.

5.1 Feedback

By following the synthesis method described in [11] a feedback controller, K_s , of third order is developed in the article [1], see Appendix 1 for exact formulation. A weighting filter is also needed in the feedback. This is a low pass filter W .

$$W(s) = \frac{10}{10 \cdot s + 1}$$

The total feedback part is thus $C = W K_s$. This is the bottom block in Figure 2 described as feedback.

The stability properties of the system is analysed by looking at the loop transfer function $L = C G_{22}$. We consider the feedback loop of Figure 2 as is shown in Figure 8. The input d is a disturbance signal.

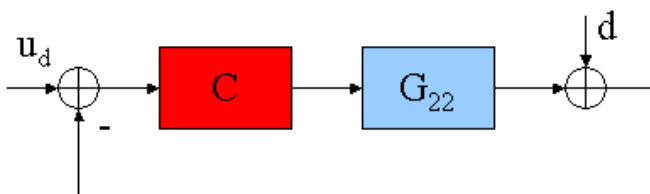


Figure 8: Feedback of the channel-steering angle to yaw rate

The Nyquist plot of the loop transfer function is used to show stability. From the control theory we know that the feedback system is stable if the Nyquist plot of L does not encircle the point -1 on the real axis.

The robustness of the model can be analysed by varying some uncertain parameters when plotting the Nyquist curve of the open loop transfer function. The model is considered robust if variations not give instability. The front and rear cornering stiffness and the speed are the parameters being varied.

Figure 9 (left) shows the Nyquist curve of the open loop transfer function when varying the front and rear cornering stiffness, C_f and C_r . The nominal value, which is pointed out, is varied $\pm 30\%$. Figure 9 (right) shows the Nyquist curve of the loop transfer function L . It is obvious that -1 isn't encircled. The blue line represents the nominal values.

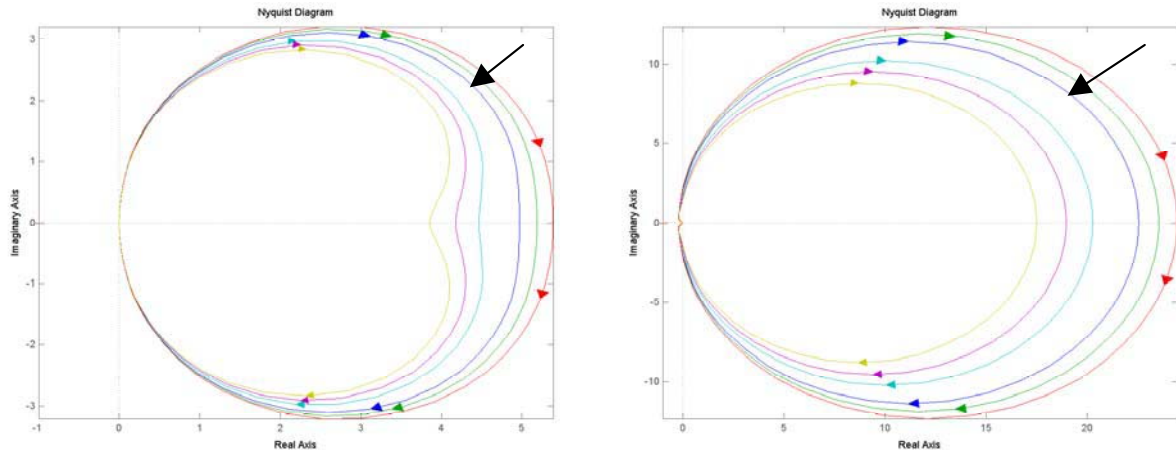


Figure 9: Nyquist curve of the; open loop transfer function (left), loop transfer function (right)

Varying the velocity attains the Nyquist curves in Figure 10, the velocity has been changed from 5 m/s to 50 m/s. Still neither the model nor the system becomes unstable.

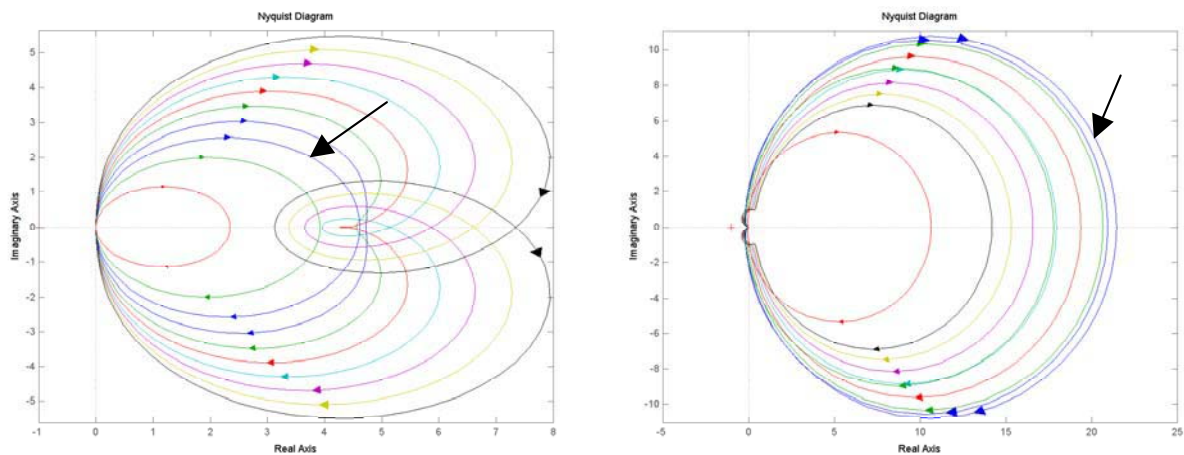


Figure 10: Nyquist curve of the; open loop transfer function (left), loop transfer function (right)

The system seems to be inherently robust, since the Nyquist curve is strictly in the right half plane. Thus Figure 9 and 10 shows that the open loop transfer function G_{22} is stable and that the feedback system is robust.

5.2 Feedforward

The feedforward part takes the steering angle performed by the driver as input and the yaw rate as the output. This part consists of two parts, the speed scheduling gain $\alpha(v)$ and the filter K_1 . The speed scheduling gain is expressed as $\alpha(v) = G_{22}(0, v) / K_1(0)$. At steady state the transfer function between u_d and r in Figure 2 is equal to the transfer function of the vehicle between u and r . This means that the controlled and the conventional vehicle have similar steady state behaviour.

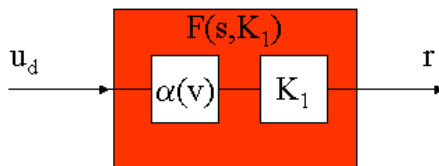


Figure 11: The feedforward part

The filter K_1 is a seventh order controller expressed in state space form in the appendix. The Bode plot in Figure 12 shows that the controller is stable and that the phase margin is about 83° .

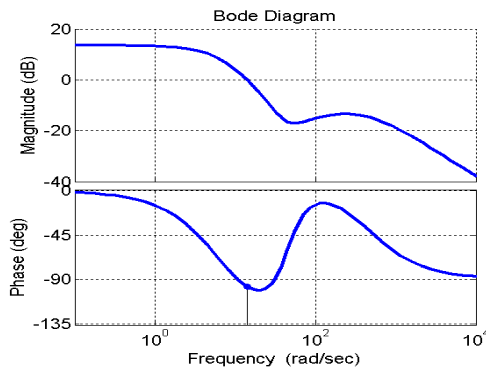


Figure 12: Bode plot of the feedforward controller $F(s, K_1)$

6 Simulations

Different simulations are done for the system to be able to decide whether stability really is improved or not by the control system. And to decide if the active steering system has a suitable response for real driving commands. Due to the delay of the active steering response a risk for driver induced oscillations exist.

Since driving is composed of an infinity of more or less different driver events and conditions it is necessary to limit the area of interest for the simulations. Two different conditions will be considered here, at-the-limit driving and nominal driving. Varying the two variables μ (road adhesion) and v (speed) attains these two conditions. The definitions of the driving conditions are arbitrary and in no way normalised.

All the simulations use the non-linear vehicle model for both the controlled and the conventional system. The steering angle, which is the steering command of the vehicle, is the angle of the front wheels. The steering angle is related to the steering wheel angle by a multiplicative factor, the steering gear ratio. The steering angle will be illustrated for all the simulations. A positive signal is a motion on the steering wheel to the left, counter clockwise.

For the conventional vehicle the steering angle is the command performed by the driver. For the controlled vehicle the steering angle is an addition of the command performed by the driver and the signal from the control system. If the illustrated steering angle is multiplied by the steering gear ratio 21 the angular movement of the steering wheel is received.

6.1 Conditions for the simulations

Nominal driving is the term used for driving at $v = 20$ m/s and $\mu = 1$.

At-the-limit driving is decided as the two cases:

$v = 40$ m/s and $\mu = 1$.

$v = 20$ m/s and $\mu = 0.3$.

The different cases, nominal and at-the-limit driving, are summarized by the following figure

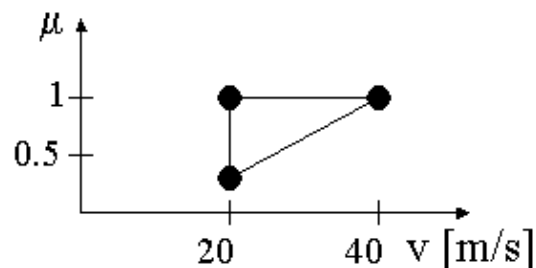


Figure 13: Friction-velocity diagram

Following simulations will be performed:

- Wind gust disturbances will be investigated assuming two cases, with driver action and without driver action.
- A severe double lane change will be simulated with the steering angle input from real driving experiments. Different velocity and road friction parameters will be considered.
- Wind force disturbance and variable changes.

All the figures containing responses of the controlled and the uncontrolled system has the controlled response depicted with a solid line and the conventional with a dotted line.

6.1.1 Driver reaction time

Driver reaction time is the time between the perception of an event that demands action and the performed action. In the case of steering, reaction time is the time when starting to correct some kind of disturbance from the surroundings. Different suggestions are described for such a reaction time in the literature, values between 0.3 and 0.6 seconds are specified. In [7] a definition and value for the reaction time is defined.

The reaction time is defined as the time range between the following two limits: 10% of the maximum wind force and 10% of the maximum steering angle performed. Experiments in [7] showed that out of twelve drivers an average value for the steering reaction time is approximately 0.3 seconds, which is the reaction time used for the thesis. Such a low level depends on that the driver is prepared of a forthcoming event.

6.2 Wind force disturbance

There are several ways to describe the influence of crosswind gusts acting on a car. In this thesis a crosswind gust is represented as force acting on the right side of the car. The force is assumed to be acting 0.4 metres in front of the centre of gravity on the right side of the car.

6.2.1 Wind force model

The wind models used for the wind disturbance event are described in Figure 14. The peak value is normalized and might be multiplied with a force value between 400 N and 1200 N according to [7]. For some simulations the curve of the crosswind model was adjusted to match a longer time interval simply by extending the steady state value.

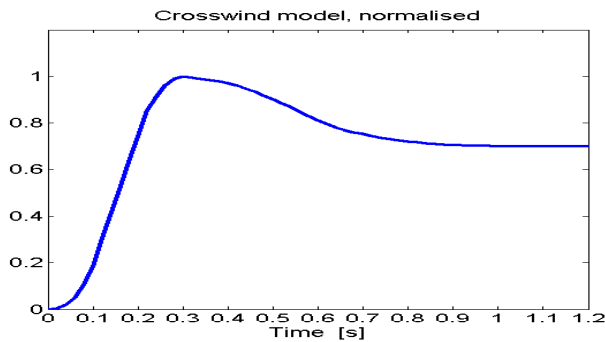


Figure 14: *Crosswind models left right*

The model in Figure 14 is called the Generalised Crosswind Model and is developed in [7]. The model has an accurate correspondence to both the lateral force and the yaw rate generated by typical crosswind gusts. One significant difference between the model in [7] and the model in this thesis is the influence of the torque caused by the wind force. Here only a linear effect proportional to the wind force is assumed but [7] shows a characteristic non-linear relation.

In the simulations a wind force with a peak value of 600 N is assumed. After peaking the wind force fades toward 420 N and then kept constant. The lateral displacement between the controlled and the conventional car due to the influence of this wind force is after 100 m approximately 4 m when no driver input is performed and nominal driving assumed.

6.2.2 Wind gust disturbance on vehicle

The figures below show the response on the vehicle due to a wind force disturbance with the appearance as Figure 14. The solid (red) line corresponds to the response of the controlled vehicle while the dotted (blue) line corresponds to the conventional vehicle. The steering angle is the signal u depicted in Figure 2.

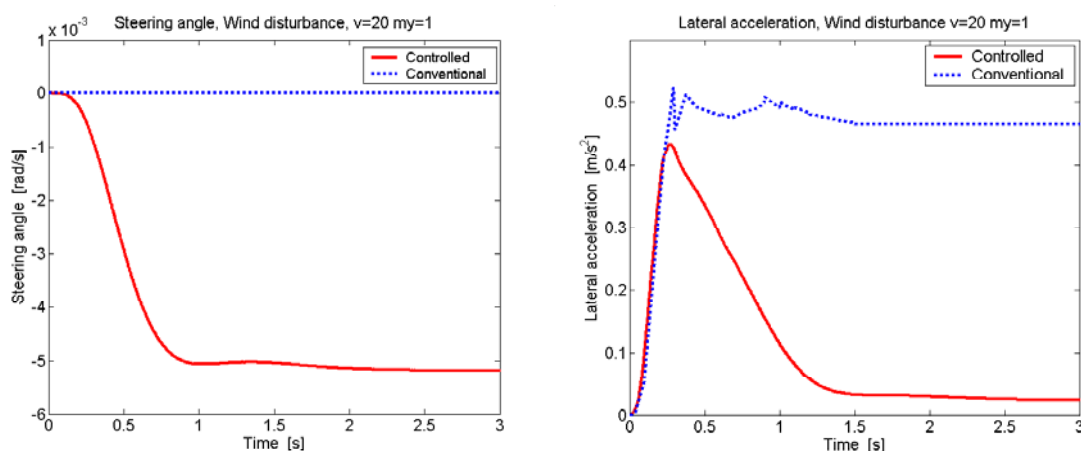


Figure15a: *Vehicle response due to wind force disturbance*

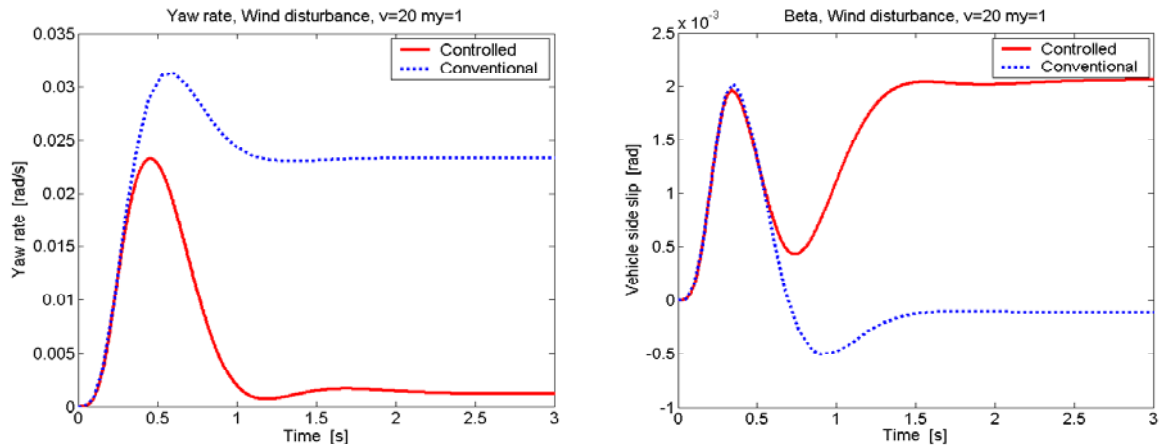


Figure 15b: *Vehicle response due to wind force disturbance*

As the left plot in Figure 15a shows the control system reacts to the wind force disturbance by adding a steering angle to the zero steering wheel input from the driver. The counteracting steering command is the reason for the decreased lateral acceleration of the car.

It is obvious that the yaw rate is attenuated for the controlled vehicle compared to the conventional and that the yaw rate during the transient phase is smaller than for the conventional car. That the yaw rate does not get zero indicates that the controlled car will move slightly to the left and therefore needs the influence of the driver to go straight.

If the definition of the reaction time, defined in section 6.1.1, is applied on the steering angle response of the controlled car, the system reaction time can be determined.

10% of Maximum steering angle after	0.25 s
10% of Maximum wind force after	0.077 s
Reaction Time	$0.25 - 0.077 = 0.17$ s

Table 5: System reaction time

Thus the system manages to act on the wind disturbance faster than a driver would but still it is uncertain if the system is fast enough to prevent the driver from taking action immediately after the disturbance. Since most of the control action (steering angle) is performed after the driver reaction time 0.3 seconds.

6.2.3 Driver in the loop

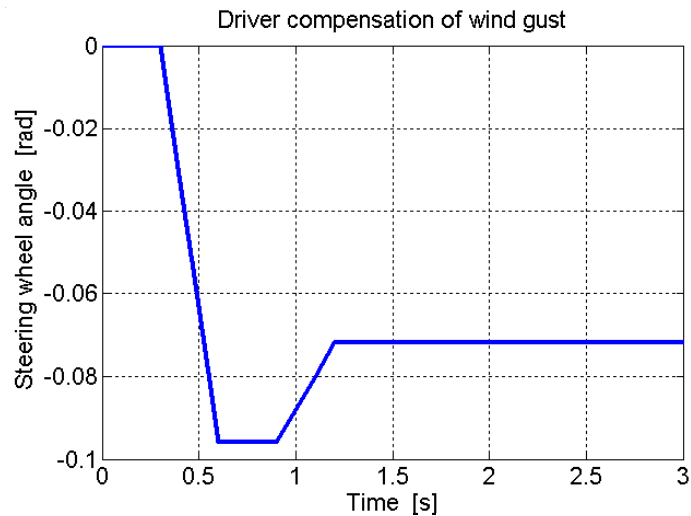


Figure 16: *Steering wheel movement to compensate for wind*

When drivers are facing wind gust disturbances some kind of compensation will take place. In [7] a suggestion of the compensating movement is presented. A simplified response will be used to simulate driver action to a wind gust. The crosswind is assumed to start at $t = 0$ and driver action to compensate for the wind starts at $t = 0.3$ s. The amplitude of Figure 16 must be adjusted to match the amplitude of the wind force. A steering gear ratio of 21 is assumed. To get the steering angle the values of the y-axis of Figure 16 has to be divided by 21.

If it is assumed that the driver takes action, to compensate for the wind force as described above, responses of the controlled vehicle can be illustrated. Both the conventional and the controlled vehicle will have similar paths. After the disturbance has taken place a delayed compensation will follow to find the right lateral position (same as before the disturbance).

The driver action is assumed to be such that the vehicle moves as straight as possible despite the wind. The maximum lateral displacement on a longitudinal distance of 200 m is 40 cm for the conventional car and 60 cm for the controlled car. This might indicate that it is a doubtful assumption that the driver in the controlled vehicle will take exactly the same kind of action to prevent the wind force as the driver in the conventional vehicle.

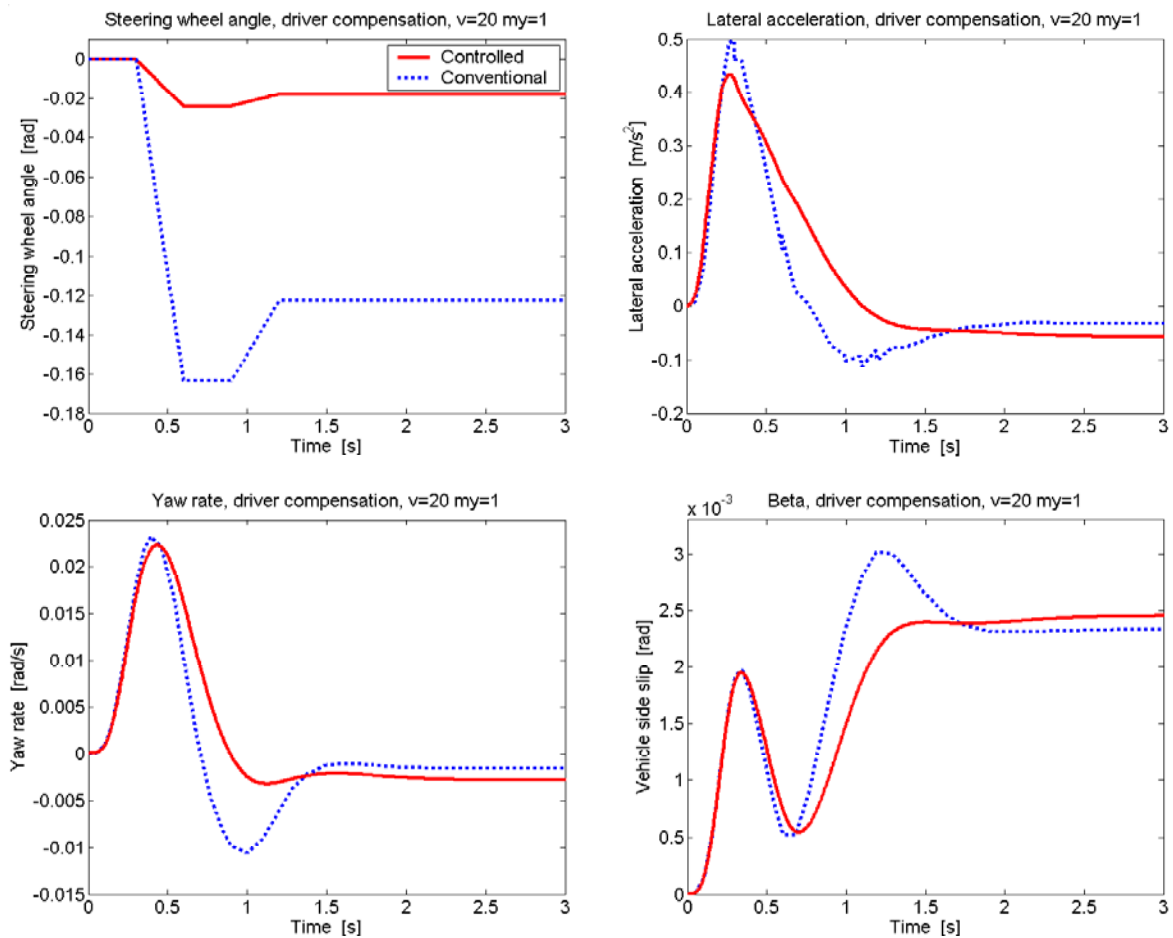


Figure 17: Vehicle responses due to wind force disturbance and driver compensation

The upper left figure shows the steering wheel angle for the controlled (red / solid) and conventional (blue / dotted) vehicle. The large difference in necessary amplitude to attain the similar road path is obvious.

A comparison between the conventional and the controlled car show that the steering wheel movement for compensation is 6.7 times larger for the conventional car.

This might indicate increased driver comfort since only very small corrections to prevent wind gust disturbances are necessary. On the other hand if the driver in the controlled car reacts the same way as the driver of the conventional car the amplitude of the driver signal will be too large and might cause dangerous situations. This is verified in simulations.

The question arises: will the driver of a car with active steering learn how to react on disturbances? This will not be further discussed here.

When the part of the steering angle coming from the control system is added to the driver's command a total signal very similar to the steering angle of Figure 15a is attained. Figure 18 shows the resulting steering angle of the controlled vehicle.

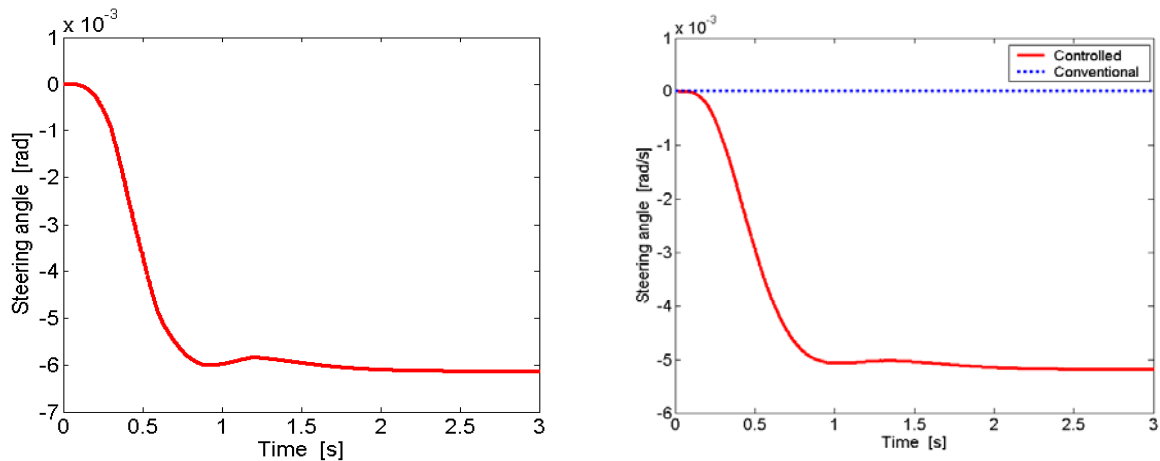


Figure 18: Steering angle of the controlled vehicle due to driver rejection of wind force disturbance Figure 13a is shown to the right

6.3 Severe double lane change

An experimental vehicle was used to perform the ISO-standardized severe double lane change. Data was collected for different speeds to be able to make the simulations. Some of the variables measured were lateral acceleration, yaw rate, steering wheel angle and longitudinal velocity. The registered steering wheel movement was then used as input to the non-linear vehicle model. A specification of the test is shown below. The test was performed with different speeds starting at 50 km/h. The road friction coefficient could be considered to be 1. Constant speed was required when entering and running through the track.

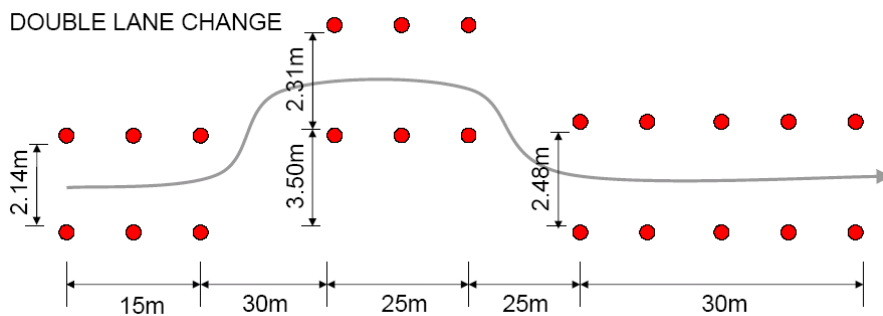


Figure 19: ISO-standard double lane change

To be able to follow the vehicle in a fictitious road path (inertial coordinate system) a transformation of the system output data (vehicle coordinate system) has to be done. A

transformation of coordinates using the transformation explained in [3] gives the right position coordinates. The coordinate transformation operator is showed below:

$$\bar{r}_I = \begin{bmatrix} \cos \psi & -\sin \psi & 0 \\ \sin \psi & \cos \psi & 0 \\ 0 & 0 & 1 \end{bmatrix} \cdot \bar{r}_M$$

Where \bar{r}_I are the position vector and the sub indices I denotes the inertial coordinate system and M denotes the vehicle coordinate system. The angle ψ is the yaw angle, which is the integration of the yaw rate.

Figure 20 below shows the road path after transforming the output data. The left figure shows the path of the non-linear vehicle model when using real steering wheel input. The input to the model is steering wheel data that has been collected from a laboratory car. The discrepancy between Figure 19 and the left figure below depends on an accumulative additive measurement error due to the equipment used. The lateral error is approximately eight meters after 200 m.

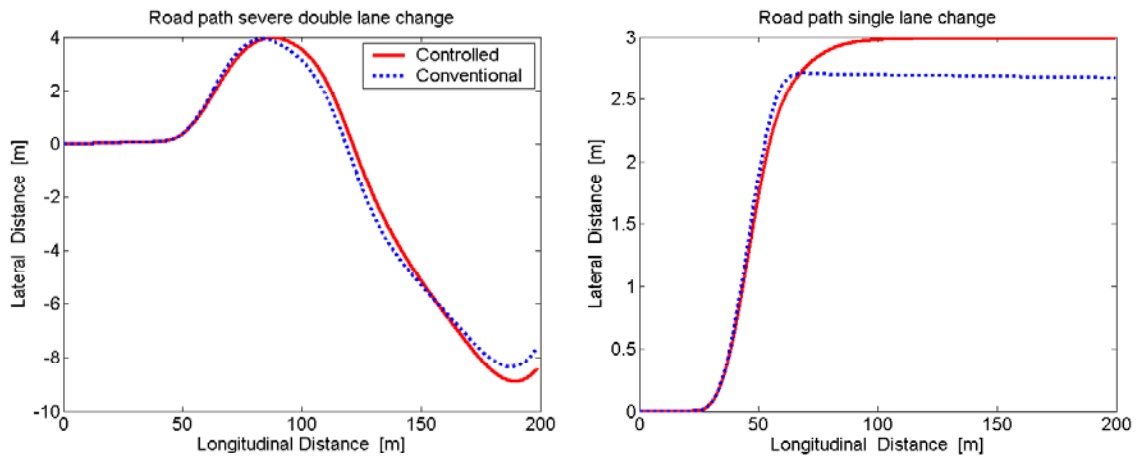


Figure 20: Road path for real input to vehicle (left), analytic input (right)

The right curve is a perfect single lane change manoeuvre [9]. This is the single sinusoidal steering wheel angle expressed in equation 17.

$$\delta_f = \begin{cases} 0.05 \cdot \sin(2 \cdot \pi \cdot 0.5(t - 0.1)) & \forall \quad 0.1 < t < 2.1s \\ 0 & \forall \quad \text{else} \end{cases} \quad (17)$$

The right figure is shown to prove that the lateral sliding of the left figure is not the result of a bad or wrong implementation. When the road position is computed two integrations are made which makes the error increase with time. This is why the lateral displacement error is maximized at the end.

6.3.1 Nominal condition

The driver steering command of a severe double lane change was used as input to the non-linear vehicle model to see if such a command delivers a proper response. The speed is considered constant throughout the manoeuvre.

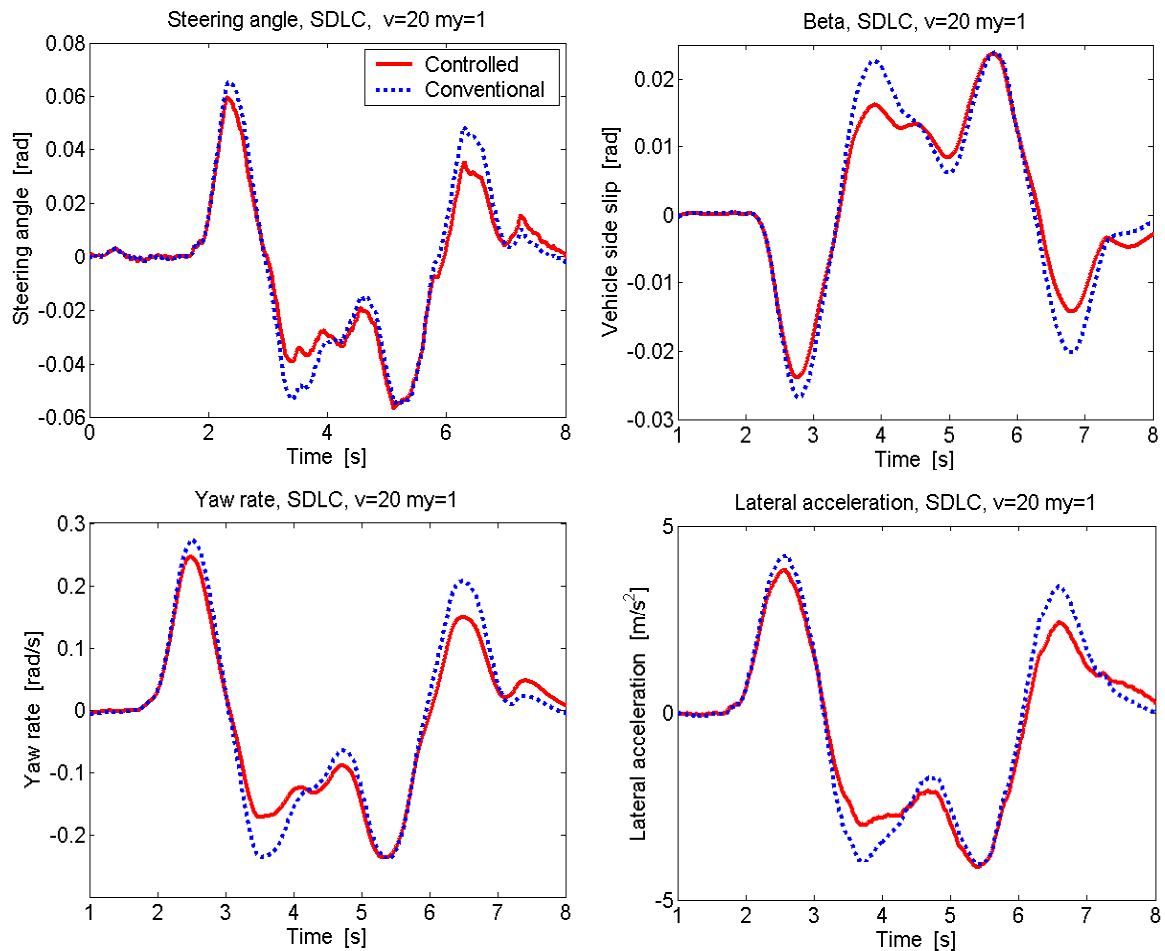


Figure 21: Severe double lane change nominal condition

An evasive movement such as the severe double lane change shows a proper response. The controller subtracts or adds a steering angle to the driver command. During the whole manoeuvre the steering angle of the controlled vehicle follows the input and therefore the yaw rate and the sideslip angle follows.

Comparing the response from the vehicle models with the data extracted from the experimental vehicle used for the driving event shows a proper correspondence. This indicates that the vehicle model used is adequate.

6.3.2 High speed

The steering command of this simulation uses the registered steering wheel movement belonging to an attempt on the track of Figure 19. This attempt was done at 110 km/h and one cone was overturned. So the input to the vehicle systems doesn't exactly correspond to the right speed.

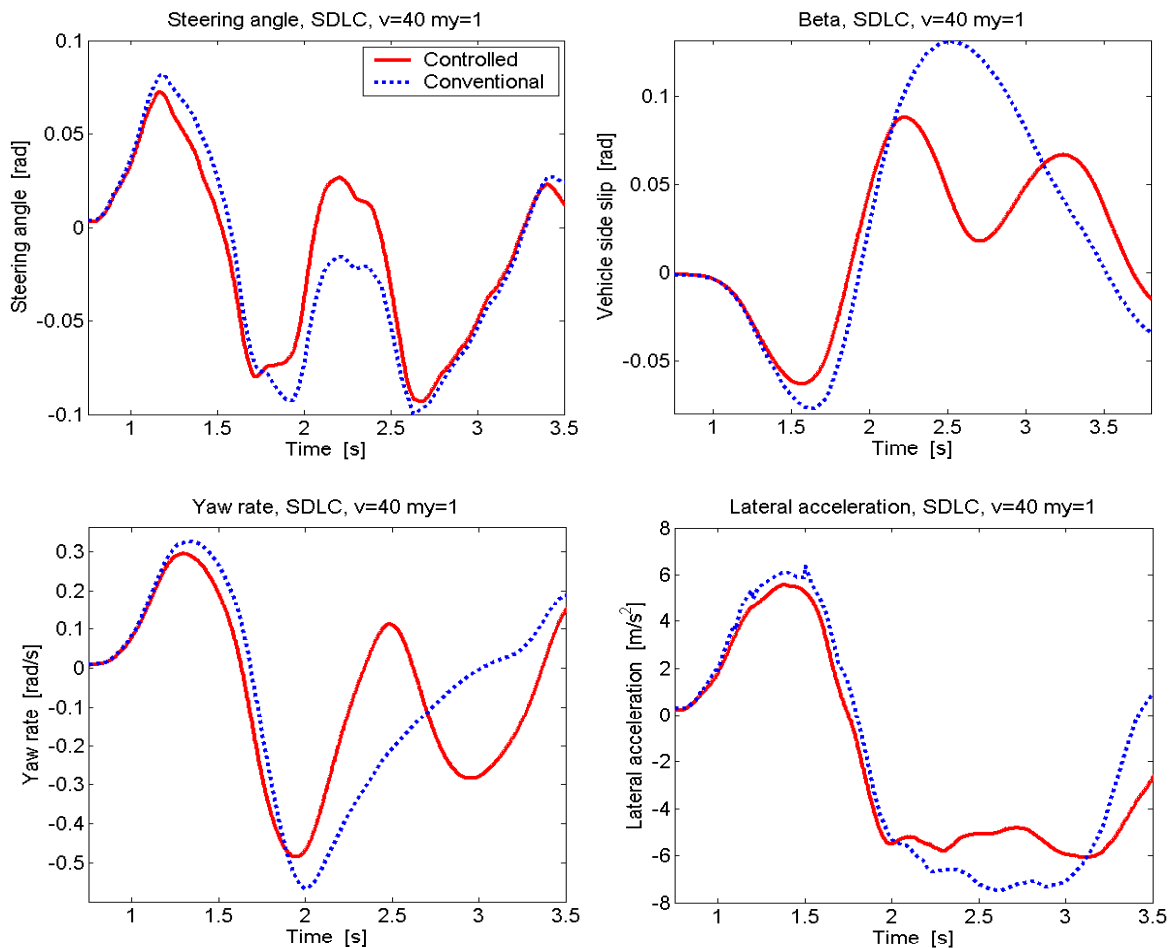


Figure 22: Severe double lane change, at the limit driving

As shown in the lower left plot of Figure 22 the yaw rate doesn't manage to follow the steering angle in the upper left figure. The yaw rate of the controlled vehicle shows better correspondence to the steering angle than the conventional vehicle. But none of the vehicles would manage the track of the severe double lane change. The response of the yaw rate and the sideslip of the conventional vehicle indicate instability.

6.3.3 Low friction

The steering command of this simulation corresponds to an experiment with the same speed, 20 m/s but with a road adhesion coefficient of approximately 1. This simulation uses a road adhesion coefficient of 0.3.

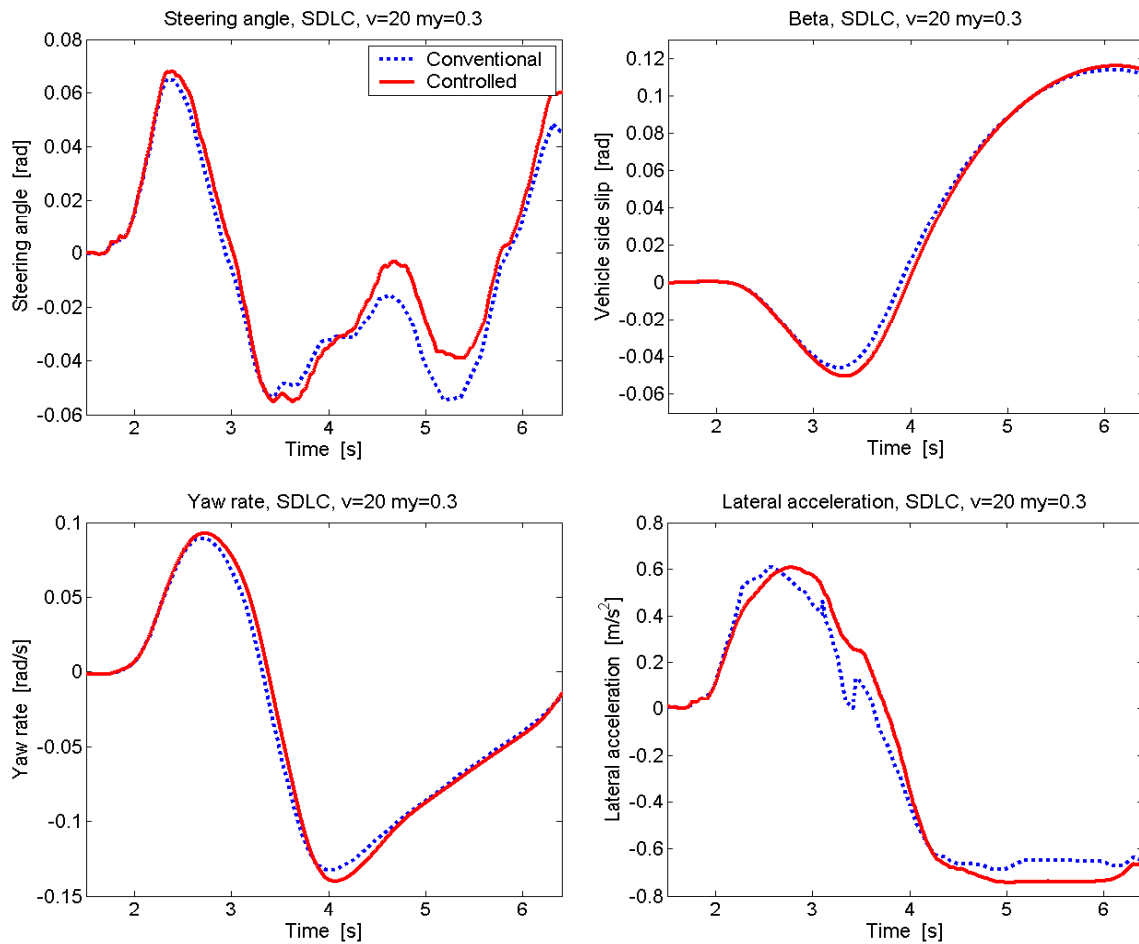


Figure 23: Severe double lane change, at the limit driving, low road adhesion

As shown in Figure 23 the yaw rate and the sideslip don't manage to follow the steering angle of the upper left plot. This indicates that the two systems become uncontrollable for this specific event and for this road adhesion level.

6.4 Wind force disturbance and variable changes

A simple way to analyse the robustness of the system is to change parameters that are considered variable or uncertain and then look at the response to see when the system gets unstable. In the following simulation the road adhesion coefficient μ and the speed v will be changed and the yaw rate will be observed. This will be done for both the conventional and the controlled vehicle as the vehicle experience a wind gust disturbance. Only one of the parameter will be changed at the time. First the speed is considered constant ($v = 20$ m/s) and μ changed. Then μ is considered constant ($\mu = 1$) and the speed increased. The speed is changed with 2 m/s from 20 to 50 m/s. μ is decreased with 0.1 steps from 1.

Figure 24 shows the conventional system.

Blue colour (the lower curves) displays the yaw rate when $\mu = 1$ and $v = 20-50$ m/s.

Black colour (the upper curves) displays the yaw rate when $v = 20$ m/s and $\mu = 1-0.3$.

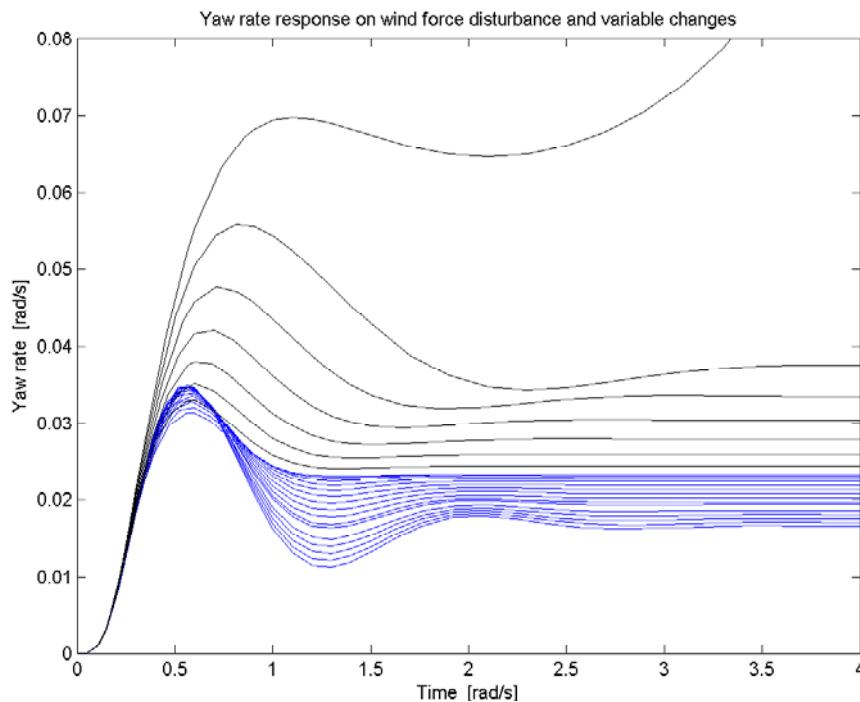


Figure 24: Yaw rate response on wind force disturbance and changes in variables for conventional system.

The figure above shows that the system doesn't get unstable by changing the speed for this specific event. The black curve however shows that decreasing μ gives more oscillation on the yaw rate and finally the vehicle becomes unstable for $\mu = 0.3$.

Figure 25 shows the controlled system.

Blue colour (the lower curves) displays the yaw rate when $\mu = 1$ and $v = 20-50$ m/s.

Black colour (the upper curves) displays the yaw rate when $v = 20$ m/s and $\mu = 1-0.2$.

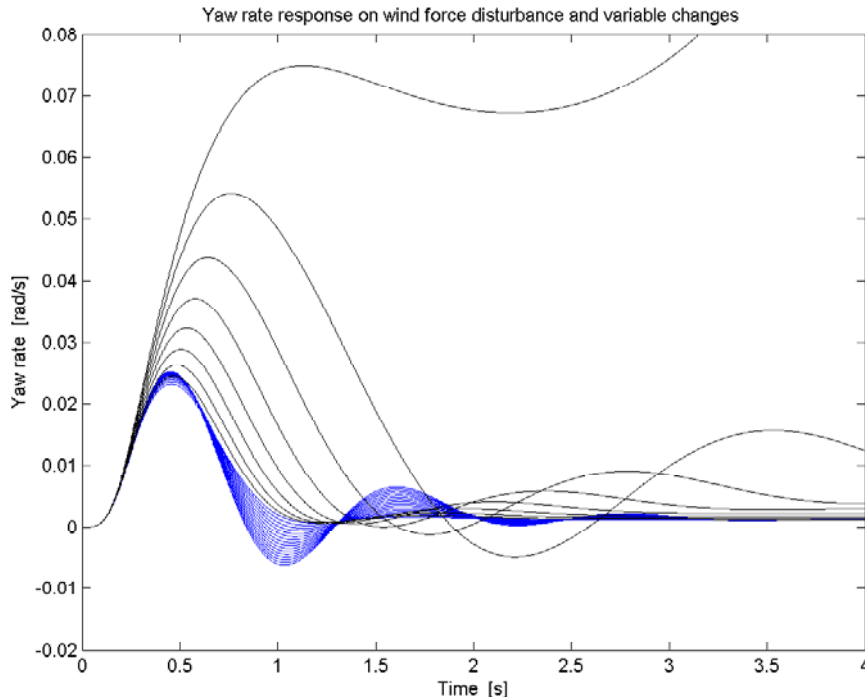


Figure 25: Yaw rate response on wind force disturbance and changes in variables for controlled system.

Figure 25 above shows that the system doesn't get unstable by changing the speed for this specific event, although the yaw rate oscillates more than for the conventional system. The black curve however shows that decreasing μ gives more oscillation on the yaw rate and finally the vehicle becomes unstable for $\mu = 0.2$.

A comparison between the controlled and the conventional system shows that the stability is increased for the controlled system. The conventional system becomes unstable for $\mu = 0.3$ and $v = 20$ m/s while the controlled system manages a lower level on μ . The controlled system becomes unstable for $\mu = 0.2$ and $v = 20$ m/s. This is true for this specific event but might indicate increased stabilisation for the controlled system.

7 Conclusion

The simulations done in chapter 6 have been performed to be able to draw conclusions on the control system. It is difficult to draw conclusions on specific simulations.

Wind force disturbance

Section 6.2.2 shows that a wind force disturbance is reduced by the control system; the yaw rate response is diminished by the control signal. About one second after the disturbance the responses are constant. Although most of the controller action takes place after driver reaction time attenuation occurs in a satisfactory way. A driver in the controlled vehicle has to take some action to straighten up the vehicle but the necessary motion will be smaller and doesn't have to be instant as for the conventional vehicle. The time range for driver action is prolonged and prevention movement reduced.

The controller reduces the lateral displacement due to a wind force disturbance. While the conventional vehicle would have a lateral displacement of 5.6 meters after 100 meters for nominal conditions, the controlled vehicle will have a lateral displacement of 1.4 meters.

Driver interaction to disturbance

If the driver senses the wind force disturbance, despite the attenuation of the yaw rate, and takes the appropriate action to prevent the forced movement, the simulation in section 6.2.3 shows that the system handles this well. The response due to driver interaction on the vehicle-control system has nice appearance. The overshoot and undershoot of the yaw rate and the sideslip angle has been slightly attenuated. The steering angle, meaning the signal from the driver added to the signal from the controller, shown in Figure 18 has a very similar appearance to the steering angle plot in Figure 15a.

The necessary movement on the steering wheel, to adjust for the wind force, is 6.7 times larger for the conventional vehicle compared to the controlled vehicle. If the drivers in both vehicles react with the same behaviour as the steering wheel angle in Figure 17 they will have practically the same path. But the comfort for the driver in the controlled vehicle is better since only a small correction is necessary.

The reactions of drivers to disturbances are difficult to anticipate but the simulation in section 6.2.3 shows that the control system handles this specific event. If the driver of a controlled vehicle should react exactly as he or she does to disturbances in a conventional vehicle the response of the vehicle could be a bit surprisingly due to the magnitude of the steering angle. The effect would be similar to an unjustified movement on the steering wheel.

Steering wheel command from measured data

The real steering wheel command in the severe double lane change returns acceptable vehicle responses. Both the vehicle model and the control system manage to handle such an evasive movement on the steering wheel. The conclusion drawn is that the control system handles real driving commands and not only fictitious test signals.

Doing the simulation for a greater velocity (40 m/s) indicates that the conventional vehicle becomes unstable faster than the controlled vehicle since the responses of the vehicle follows the steering angle command better.

Doing the simulation for smaller road adhesion coefficient (0.3) shows clearly that the lateral forces of the vehicle aren't enough, neither for the controlled nor the conventional vehicle, for the vehicle responses to follow the steering angle. Both systems are obviously uncontrollable at these conditions. Of course if the speed is decreased the yaw rate will start to follow the steering angle input at this road adhesion level.

The response of the yaw rate and the vehicle sideslip vary in a good manner due to different road adhesion levels and different speeds. This is not showed in the report but it is a clear confirmation that the introduction of the friction in the vehicle model is done properly.

Stability increase

The last simulation in the report shows that the conventional vehicle gets unstable faster than the controlled vehicle when a wind force disturbance is experienced and the road adhesion coefficient is decreased. Figure 24 and 25 clearly shows that the conventional vehicle becomes unstable at $\mu = 0.3$, while the controlled system becomes unstable at $\mu = 0.2$ for the same disturbance.

This indicates that the control system increases the stability area of the vehicle when there is no driver action on the steering wheel.

Are the goals fulfilled?

The goals of the thesis where to:

Characterise the difference of the response between the controlled and the uncontrolled vehicle for nominal driving and at the limit driving.

For nominal driving the response between the two systems is quite similar but for situations other than nominal ones some differences are obvious. Simulations have shown that the yaw rate follows the steering angle closer for certain events such as the severe double lane change during high speed. When the road adhesion gets to low the lateral forces are not enough for the yaw rate to follow the steering angle and not even the control system handles that. For this case the yaw rate response is very much the same for both systems.

Establish whether the system is considered to act within driver reaction time.

It is established that the control system reacts almost twice as fast as a human driver to the wind force disturbance. But it should be considered that most of the control action is taken place after the driver reaction time. Corrections made by the driver in the controlled system will have to correct the lack of controller ability to remove disturbances. My opinion is that the control system prolongs the available reaction time on a specific disturbance.

Have a system with steady state rejection or attenuation of input disturbances.

The system clearly reduces the effect of the wind force disturbance, but a small remaining error still exists in steady state. This could easily be removed by changing the filter W in the feedback loop. But a small error is no big problem due to the correction of the driver.

Prove enhancement of the stability region.

It is shown that the controlled vehicle is harder to make unstable than the conventional one. For certain events, such as the wind force disturbance, a lower level on the road adhesion is possible for the controlled vehicle. Also at higher velocities than the nominal, the controlled vehicle shows better controllability than the conventional one.

Future work

The future work could be to implement the active steering system in an experimental car. Most suitable would be a car with steer-by-wire. Implementation in a car is the only true way to examine the perception of the feeling of the driver. An implementation in a real car demands changes in the system so that for example speed variations are considered. Since the transfer function of the vehicle is dependant of the velocity. How the extra steering angle should be delivered is also an important problem to solve.

Another way to continue this thesis is to test the system on different vehicle models to examine the responses further.

8 References

- [1] Mammar S. Koenig D.: *Vehicle Handling Improvement by Active Steering*. Vehicle System Dynamics, Vol. 38, No. 3, pp 211-242.
- [2] Kiencke U. Nielsen L.: *Automotive Control Systems for Engine, Driveline and Vehicle*. Springer kap. 6.
- [3] Wennerström E. Nordmark S. Thorwald B.: *Fordonsdynamik*. KTH, Stockholm 1999.
- [4] Pacejka H.B.: *Tyre and Vehicle Dynamics*. BH
- [5] Glad T. Ljung L.: *Reglerteknik Grundläggande teori*. Studentlitteratur.
- [6] Glad T. Ljung L.: *Reglerteori Flervariabla och olinjära metoder*. Studentlitteratur.
- [7] Jarlmark J.: *Driver-vehicle interaction under influence of crosswind gusts*. Lic. Thesis, KTH, Stockholm 2002.
- [8] Mammar S. Baghdassarian V. B.: *Two-degree-of-freedom Formulation of Vehicle Handling Improvement by Active Steering*.
- [9] Ackermann J. Bünte T.: *Handling improvement of robust car steering*. International Conference on Advances in Vehicle Control and Safety, Amiens, France, 1998
- [10] Åström K. J.: *Control system design*.
<http://www.cds.caltech.edu/~murray/courses/cds101/fa02/caltech/astrom.html>
- [11] www.sae.org/automag/techbriefs/01-2001/techb2.htm 040212
- [12] SIP: Utbildnings- och informationsprogram BMW Group 03/2003

Glossary

Yaw rate - See definition below.

Vehicle sideslip angle - Lateral velocity divided with longitudinal velocity.

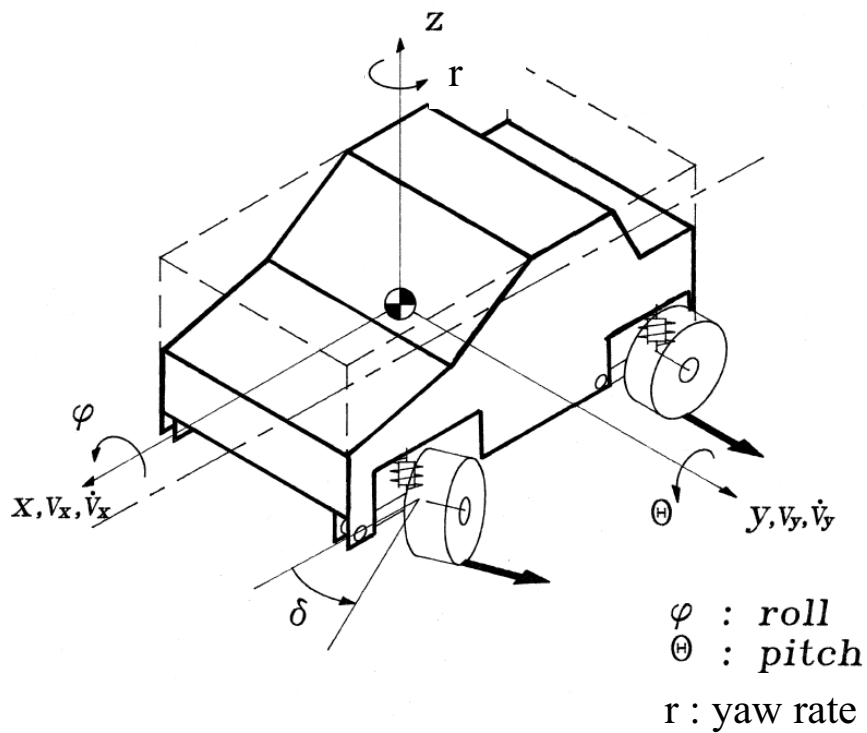
Cornering stiffness - The change in lateral force per unit slip angle change in the linear range.

Roll - The rotation of the vehicle about its longitudinal axis.

Bounce - Vehicle motion perpendicular to the ground.

Pitch - The rotation of the vehicle about its lateral axis.

SBW - Electrical steering that replaces the mechanical steering control.



Appendix

Feedback controller in state space form

$$K_s = \begin{bmatrix} A_s & B_s \\ C_s & D_s \end{bmatrix} = \left[\begin{array}{ccc|c} -4.476 & -75.091 & 26.229 & -74.159 \\ 17.198 & -1104.9 & 332.42 & -1100.4 \\ -3.321 & -165.03 & -70.256 & -158.01 \\ \hline 0.4152 & 0.8764 & 7.532 & 0 \end{array} \right]$$

Feedforward controller in state space form

$$K_1 = \begin{bmatrix} A_1 & B_1 \\ C_1 & D_1 \end{bmatrix}$$

$$A_1 = \begin{bmatrix} 0.0456 & 0.4922 & 3.6785 & -0.6176 & -2.3028 & -0.0991 & 0.0413 \\ 0.4955 & -0.4167 & -4.5084 & 0.7342 & 2.8425 & -0.4207 & 0.3681 \\ 0.0930 & -0.1865 & -1.7029 & 0.2729 & 1.0697 & -0.0586 & 0.0632 \\ -0.1473 & 0.2322 & 2.3201 & -0.4984 & -1.4394 & 0.0859 & -0.0925 \\ 0.2604 & -0.2440 & -2.5935 & 0.4471 & 1.6226 & -0.2169 & 0.1891 \\ 0.5903 & 0.3068 & 0.7899 & -0.1420 & -0.4767 & -0.5891 & 0.4399 \\ -0.2031 & -0.2894 & -1.6953 & 0.2837 & 1.0560 & 0.2150 & -0.1598 \end{bmatrix}$$

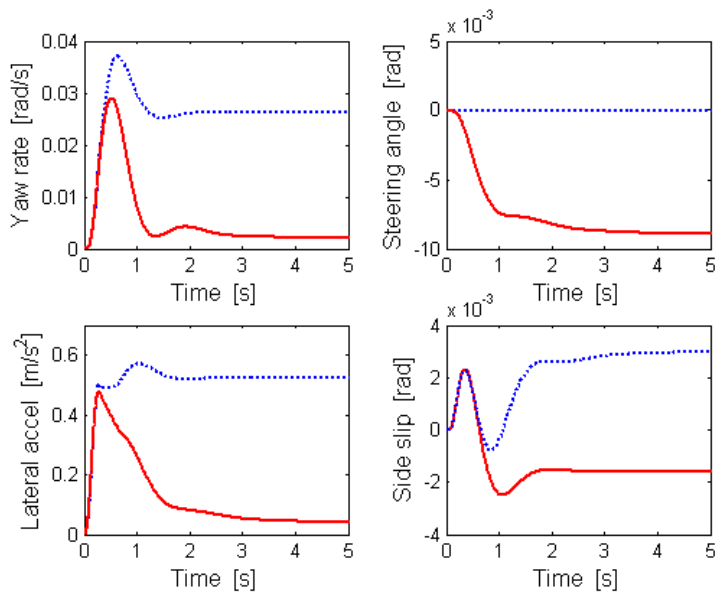
$$B_1 = \begin{bmatrix} 2.3586 \\ -2.6134 \\ -0.3260 \\ 0.1738 \\ -0.9865 \\ 1.2941 \\ -27.3612 \end{bmatrix}$$

$$C_1 = \begin{bmatrix} -32.1898 & -11.7928 & -0.4920 & -7.1839 & 0.9547 & 29.1518 & -22.2469 \end{bmatrix}$$

$$D_1 = 0$$

Simulations for Saab 9-5 characteristics: Wind gust disturbance

$V=20$ m/s and $\mu=1$



Simulations for Saab 9-5 characteristics: Severe double lane change

$V=20$ m/s and $\mu=1$

